1-1-2021

Nudging the N170 forward with prior stimulation—Bridging the gap between N170 and recognition potential

Canhuang Luo
Hangzhou First People's Hospital

Wei Chen
Khalifa University of Science and Technology

Rufin VanRullen
Universite Paul Sabatier Toulouse III

Ye Zhang
Hangzhou First People's Hospital

Carl Michael Gaspar
Zayed University, carl.gaspar@zu.ac.ae

RESEARCH ARTICLE

WILEY

Nudging the N170 forward with prior stimulation—Bridging the gap between N170 and recognition potential

Canhuang Luo[1,2,3,4,5] | Wei Chen[6] | Rufin VanRullen[4,5] | Ye Zhang[1,2,3] | Carl Michael Gaspar[1,2,3,7]

[1]Center for Cognition and Brain Disorders, The Affiliated Hospital of Hangzhou Normal University, Hangzhou, China

[2]Institute of Psychological Sciences, Hangzhou Normal University, Hangzhou, China

[3]Zhejiang Key Laboratory for Research in Assessment of Cognitive Impairments, Hangzhou, China

[4]Université de Toulouse, UPS, Centre de Recherche Cerveau et Cognition, Toulouse, France

[5]CerCo, CNRS UMR 5549, Toulouse, France

[6]Khalifa University of Science and Technology, Abu Dhabi, United Arab Emirates

[7]Zayed University, Abu Dhabi, United Arab Emirates

Correspondence
Carl Michael Gaspar, Department of Psychology, College of Natural and Health Sciences, Zayed University, PO Box 144534, Abu Dhabi, United Arab Emirates.
Email: carl.gaspar@zu.ac.ae

Ye Zhang, Center for Cognition and Brain Disorders, The Affiliated Hospital of Hangzhou Normal University, 311121 Hangzhou, Zhejiang, China.
Email: zhye@hznu.edu.cn

Abstract

Evoked response potentials are often divided up into numerous components, each with their own body of literature. But is there less variety than we might suppose? In this study, we nudge one component into looking like another. Both the N170 and recognition potential (RP) are N1 components in response to familiar objects. However, the RP is often measured with a forward mask that ends at stimulus onset whereas the N170 is often measured with no masking at all. This study investigates how inter-stimulus interval (ISI) may delay and distort the N170 into an RP by manipulating the temporal gap (ISI) between forward mask and target. The results revealed reverse relationships between the ISI on the one hand, and the N170 latency, single-trial N1 jitter (an approximation of N1 width) and reaction time on the other hand. Importantly, we find that scalp topographies have a unique signature at the N1 peak across all conditions, from the longest gap (N170) to the shortest (RP). These findings prove that the mask-delayed N1 is still the same N170, even under conditions that are normally associated with a different component like the RP. In general, our results suggest greater synthesis in the study of event related potential components.

KEYWORDS
Chinese characters, ERP, N170, object recognition, recognition potential, visual masking

1 | INTRODUCTION

Event-related potential (ERP) components are important for inferring the time course of perceptual and cognitive processing (Carreiras, Armstrong, Perea, & Frost, 2014; Dien, 2009; Grainger & Holcomb, 2009). The most typical type of component, the kind studied in this article, is a peak in the evoked response, which can be either a positive or negative deflection. Inference about processing can be relatively straightforward when components are classified almost exclusively by the stimulus conditions leading up to that component. In this case, delays and distortions in the component are interpreted as delays and distortions in processing. This is certainly the case with components like the readiness potential (Libet, Libet, Gleason, Wright, & Pearl, 1993) and the mismatch negativity (MMN) (Näätänen, Gaillard, & Mäntysalo, 1978). The MMN is a response evoked by an unexpected stimulus in a sequence of regularly occurring stimuli. Importantly, an early MMN evoked by auditory stimuli is just as much an MMN as a late MMN evoked by visual stimuli (Winkler, Czigler, Sussman, Horváth, & Balázs, 2005).

However, confusion can arise when components are also classified by their morphology—their latency and shape. The importance of latency in defining some components is often reflected in component nomenclature like N170 (Bentin, Allison, Puce, Perez, & McCarthy, 1996), which refers to a negative deflection occurring around 170 ms after an object from a familiar category appears. In some cases, peaks that are offset in time (with longer latencies in most cases) and slightly different in shape are thought to reflect different processes (Eimer, 2000; Martin-Loeches, Hinojosa, Gomez-Jarabo, & Rubia, 2001). While that interpretation is consistent with a cascade across processing levels, an equally valid interpretation of peak offset is a delay in processing. How can we decide between these two interpretations? This article reports unique support for the delay interpretation in a comparison between two nominally different ERP components: the N170 and the recognition potential (RP) (Martin-Loeches et al., 2001; Rudell, 1991). The approach we take arises from the possibility that the presence of forward masking during typical recordings of RP can lead to processing delay relative to the N170, which rarely involves forward masks. Masks are typically random patterns and so their mere presence is unlikely to involve a dramatic switch in processing. In order to test our delay hypothesis, we simply nudge the N170 into an evoked response that is morphologically equivalent to an RP, by using forward masks with progressively smaller inter-stimulus interval (ISI). Importantly, the experimental conditions at the extreme ends of our parametric manipulation match the conventional experimental designs of N170 and RP studies. The remainder of the Introduction describes N170 and RP in greater detail and motivates their comparison despite being studied in different literatures with very little cross talk. Experimental design is elaborated upon and more precise predictions are made in the context of the delay hypothesis.

The N170 is the first negative deflection in response to visually observed objects from a familiar category, like faces. It is described as being a critical temporal marker for the extraction of information from visually observed familiar objects (Bentin et al., 2007; Dering, Martin, Moro, Pegna, & Thierry, 2011; Dering, Martin, & Thierry, 2009;

Martín-Loeches, 2007; Maurer, Zevin, & McCandliss, 2008; Tanaka & Curran, 2001; Thierry, Martin, Downing, & Pegna, 2007a, 2007b). However, the latency of N170 can be influenced by an overlooked factor—ISI. In a survey, we made of the N170 literature (Figure 1), one can see a monotonic relationship between N170 latency and ISI (Cao, Jiang, Li, & He, 2014; Fu, Feng, Guo, Luo, & Parasuraman, 2012; A. Harris & Nakayama, 2007; Kuehl, Brandt, Hahn, Dettling, & Neuhaus, 2013; Shen et al., 2017). Additionally, in the four forward masking studies that also used short ISI, their N170 seems not only to have longer latencies than the typical N170, but are also distorted or even abolished to the extent that the latencies are difficult to estimate from the figures (Harris, Te Wu, & Woldorff, 2011; Lin et al., 2011; Martens, Schweinberger, Kiefer, & Burton, 2006; Su, Mak, Cheung, & Law, 2012). In fact, a very short ISI can delay the N170 up to ∼80 ms later than the typical latency. Taken together, the results drawn from these separate studies suggest that the N170 can be nudged forward and widened by the recency of prior stimulation. The most extreme delay should occur with zero ISI (e.g., Su et al., 2012), at which point the N170's morphology might be indistinguishable with another ERP component: the RP.

RP is usually studied in a totally separate body of literature focusing on the time course of word recognition (Dien, 2009; Martín-Loeches, 2007). Unlike the N170, the RP is usually measured with a paradigm called rapid stream stimulation (RSS) which presents multiple masks before a target in succession and multiple masks after. However, RP is similar to N170 in many other aspects. Primarily, both the RP and N170 are responses to the visual presentation of familiar objects. And there are also a number of morphological similarities between these two ERPs. Both of them are almost always N1 components (for a non-N1 RP, see Rudell, 1991; Rudell & Hu, 2010). Both ERPs are observed at similar channels and have similar topographies (Bentin, Mouchetant-Rostaing, Giard, Echallier, & Pernier, 1999; Hinojosa, Martín-Loeches, Gómez-Jarabo, & Rubia, 2000; Martín-Loeches, Hinojosa, Fernández-Frías, & Rubia, 2001; Martin-Loeches et al., 2001; Maurer, 2008; Maurer, Brandeis, & McCandliss, 2005; Maurer et al., 2008). The one major morphological difference between N170 and RP is delay: the RP typically occurs around 250 ms post-stimulus, which is longer than the typical latency of N170. And because of the delay, RP is often linked to higher level processing stages than the processing stage revealed by N170 (Dien, 2009). However, this widely accepted interpretation of RP does not consider the presence of forward masking during typical recordings of RP. If the forward mask merely delays the brain signal in response to the target, could the RP just be a delayed brain response such that its mask-free latency would actually be ∼170 ms? To put it simply, is RP actually an N170 delayed by forward masks?

Taken together, our study aims to answer two questions: (a) is the N1 systematically delayed and warped by ISI? and (b) is RP a delayed version of N170? Answers to these questions can only be obtained by establishing the relationship between ISI and N170. In this study, we measure electrophysiological responses evoked by Chinese characters, and we focus mostly on characteristics of the N1 and vertex positive potential (VPP). VPP is measured at a vertex channel

FIGURE 1 Summary of studies that used short inter-stimulus intervals (ISIs)
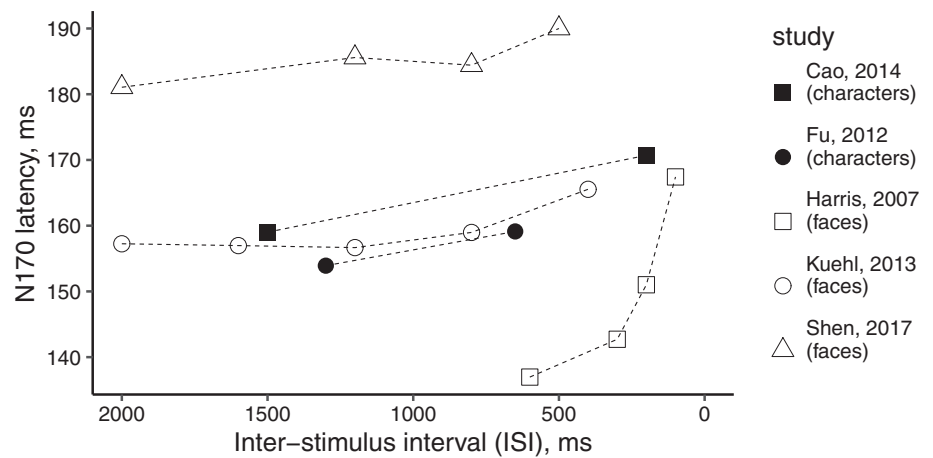
such as Cz or Fz and is considered to reflect the same process the N170 does (Joyce & Rossion, 2005; Taylor, Itier, Allison, & Edmonds, 2001). Our subjects also performed a one-back task on Chinese characters, and we measured their reaction times (RTs). In these respects, our study is like many others in both the N170 and RP literatures. However, our study is unique in three ways: First, across 14 conditions, we parametrically manipulate the temporal proximity between the target and a forward-mask image, from zero-gap (quasi-RP condition; gap denotes ISI) to infinity-gap (or no-mask, the typical N170 condition). Second, we focus on the specification of waveform-morphology in order to determine whether the N1 component obtained in N170 and gap conditions is the same. Finally, we obtain lots of data for each subject (150 trials for each of the 14 conditions). Altogether, we are able to obtain unique "gap-metric" functions, the ERP-component equivalent of a psychometric function for three major aspects of N1 morphology: N1 latency, N1 single-trial jitter, and topographical similarity to the N170. In addition, RTs measured across gap conditions also allows us to assess the functional consequences of gap-related waveform changes. Our experimental design allows us to isolate the effect of a single masking stimulus on variability in N1 morphology. All these allow us to answer the first question and part of the second question. Considering that applying only one forward mask per trial is not typical in the majority of RP studies (but see Dien, Brian, Molfese & Gold,2013), to completely answer the second question, typical RP was also measured with the RSS paradigm as a control condition and compared with all the other 14 conditions.

2 | MATERIALS AND METHODS

2.1 | Participants

Nine healthy adult participants (all right-handed, age ranging from 24 to 27, four males) with normal or corrected-to-normal vision took part in the study and were paid for their participation. Data from two participants were rejected due to too many artefact-contaminated trials (e.g., eye blinks, head movements, etc.). Valid data from seven

participants were reported here. All participants were native Chinese who had more than 10 years of education in speaking and reading Chinese characters. Written informed consent was obtained from each participant prior to the experiment.

2.2 | Stimuli

Stimuli were grey scale images of 150 Chinese noun characters and 150 masks. Chinese characters were chosen from the Modern Chinese Corpus of Center for Chinese Linguistics (Peking University, 2015) (see http://ccl.pku.edu.cn:8080/ccl_corpus/index.jsp?dir=xiandai). The frequency of each character was higher than 105 occurrences per million in this corpus, and mean frequency of all characters was 250.95 occurrence per million. The number of strokes in Characters ranged from 7 to 12 (mean 9.18). The masks were made up of the 150 Chinese characters by cutting these characters into 16 portions vertically and randomly permuting their horizontal position. These masks and Chinese characters were matched in visual attributes. The size of the basic set of characters and masks were around $4.4° \times 4.4°$ of visual angle, and the Weber contrast of the stimuli was -0.998.

2.3 | Procedure

After electrode-cap placement, participants were seated in a dim light and sound-attenuated shielded room, at a viewing distance of 60 cm from the computer monitor. Stimuli were presented with MATLAB (MathWorks, Natick, MA) using the Psychophysics Toolbox (Version 3.0.12; http://psychtoolbox.org) (Brainard, 1997; Kleiner et al., 2007) on a light grey background with luminance of 66 cd/m^2.

The sequence of events for each trial, summarised in Figure 2, is as follows: In each trial, a "+" fixation of 0.15 visual degree was presented at first in the centre of the screen for 500 ms, which was followed by a blank for 800 ms. Then, a forward mask, a character, and a backward mask were presented sequentially, each displayed for 250 ms. Each trial was ended by a blank of 800 ms. The masks in each
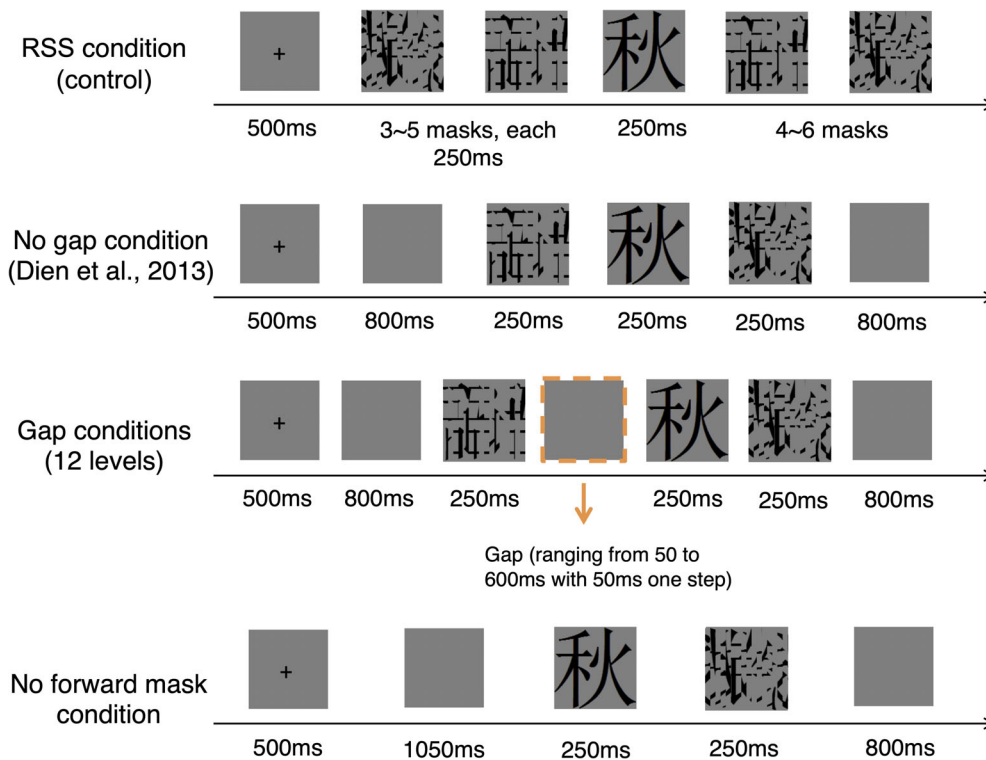
trial were randomly chosen from all the masks. Participants were instructed to make a response by pressing the "m" key as quickly and accurately as possible when a repeated character was detected in successive trials. The ISI (i.e., temporal gap) between the preceding mask and the character varied from 0 to 600 ms with a step of 50 ms. So, there were 13 gap conditions in total. Additionally, there were two more conditions. One additional condition elicited the classic N170 (no-mask condition) as there were no display of masks preceding the target (the blank interval between the fixation and the character was 1,050 ms). The other additional condition used the RSS paradigm, in which three to five masks were presented prior to the targets and four to six masks were presented after to elicit typical RP (RSS condition), which served as a control condition. The stimulus presentations for different conditions are described in Figure 2. All 15 conditions were blocked; that is, each block had only one condition. There were 58 trials in each block where 8 characters were randomly chosen to be repeated "targets" (same character as shown on previous trial). Each condition was tested with three blocks, totally 174 trials for one condition. The experiment started with a practice block of 58 trials (these stimuli were not used in the main test). The order of blocks and trials in each block were randomised, and the RSS condition (control) was conducted after the subjects completed all the other conditions.

2.4 | EEG recording and preprocessing

Brain electrical activity was recorded from 32 scalp sites using tin electrodes mounted in an elastic cap (BrainAmp, Brain Product). Vertical and horizontal eye movements were monitored using two electrodes placed on the outer canthus of right eye and in the inferior areas of the left orbit. The ground electrode was placed along the midline, ahead of Fz, and impedances were systematically kept below 7 kΩ. Signals were digitised at a sampling rate of 500 Hz and band-pass filtered at 0.016–70 Hz. Potentials were referenced on-line to the FCz electrode and averaged-referenced off-line. Participants were asked to minimise eye movements, head movement, and swallowing during the recording.

EEG data were low-pass filtered at 30 Hz and high-pass filtered at 0.1 Hz. Data were epoched from 1,000 ms before the onset of stimulus to 1,000 ms after the onset of stimulus. Only non-repeated trials were extracted. Artefact rejections were applied over the epoched data. Trials with strong α wave and abnormal trend and blink during the presentation of stimuli were rejected by visual inspection. We removed the trials containing strong α waves because, according to the participants' feedback, a few participants had a couple moments of sleepiness. Therefore, we consider a sudden increase of α power in several trials compared to most trials as a marker of sleepiness (Woodman, 2010). After trial rejection, the remaining numbers of trials did not vary much across conditions (see Table 1). Number of behavioural responses of each condition was listed in the Supplementary Table 1.

2.5 | Analysis

2.5.1 | N1 latencies (mean ERP)

The peak latencies and amplitudes of N1 were automatically extracted at the maximum (negative) amplitude value between 130 and 330 ms

TABLE 1　Number of trials per condition, summarised by minimums and maximums across subjects

	RSS	0	50	100	150	200	250	300	350	400	450	500	550	600	N170
Minimum	116	98	117	123	118	104	124	88	108	108	111	99	122	118	105
Median	138	136	136	136	134	136	138	134	138	139	134	142	140	140	133
Maximum	145	144	146	148	145	145	147	147	146	146	146	147	147	148	146

Abbreviation: RSS, rapid stream stimulation.

at P7 electrode (left occipito-temporal area), and the peak latencies and amplitudes of VPP were automatically extracted at the maximum (positive) amplitude at Fz electrode (fronto-central area) within the same time window. Automatic extraction was performed using ERPLAB (Lopez-Calderon & Luck, 2014) and EEGLAB functions (Delorme & Makeig, 2004). All the subsequent analyses, except the analyses for P1, are based on N1 at P7. We chose P7 because the maximum amplitude of N1 occurs mostly at P7 and P8 (Luo, Chen, Zhang, & Gaspar, 2019), and the left hemisphere ventral occipito-temporal cortex is involved in character or word processing (Krafnick et al., 2016).

2.5.2 | N1 widths (single-trial jitter)

N1 component width, measured directly on the mean ERP waveform, is difficult to define. Some subjects lack distinctive peaks around the N1 (P1 and P2) to serve as delimiters. Also, subjects vary in the shape of their N1 component; some having more kurtosis than others, and others being more asymmetrical. Therefore, we measured single-trial N1 components and take the *SD* of their latencies across trials—their temporal jitter—to be a proxy measure of component width. We measured the jitter in a 150 ms time window centred on the average ERP peak of each condition. Several studies have used this method to establish reliable differences in N1 latency variability across experimental conditions (e.g., Navajas, Ahmadi, & Quian Quiroga, 2013; Yang et al., 2017; Zhang, Luo, & Luo, 2013), and across subject populations (Milne, 2011). Single-trial N1 peaks were estimated from 150 ms windows centred on the latency of the N1 in the mean ERP of the appropriate gap condition and subject. Within each window of each trial, we used custom MATLAB scripts and publicly available MATLAB code to estimate the latency of the most negative local peak (findpeaks.m, authored by Prof Tom O'Haver at University of Maryland, Version 6.0, Last revised March 2016; http://terpconnect.umd.edu/~toh/spectrum/findpeaks.m).

2.5.3 | Decay function relating N1 latency and jitter, to gap

We used the following exponential function to relate both N1 latency, and N1 jitter, to gap, separately for each subject:

$$y = m * e^{-\frac{g}{k}}$$

where y can be either N1 latency (ms), or N1 jitter (*SD*, ms), g is gap (ms), m specifies the starting point (y at gap 0), and k is the inverse of the decay rate (small k means fast decay). Best fitting parameters were obtained by minimising the sum-of-squares error using MATLAB's fminsearch.m (MATLAB R2014a).

2.5.4 | Statistical analyses of correlations

Analyses of RT reported in this article used median RT; we redid all RT analyses using mean RT and the pattern of results (see Supplemental Material), including statistical significance, was the same. For statistical analyses of correlations between N1 latency and RT, and between N1 latency and VPP latency, we used the lmer program of the lme4 package (Bates, Mächler, Bolker, & Walker, 2014) for estimating fixed and random coefficients (subjects). Our focus is on the coefficient between N1 latency and RT, or between N1 and VPP latencies, modelled as fixed effects in separate models. Variation in intercept across subjects is modelled as a random effect; hence, the use of a linear mixed model (LMM). Our main results concern the coefficient associated with our fixed effects, which is evaluated in two ways. First, we examine an ANOVA-based model comparison between a subjects-only model and the subjects-plus-coefficient model (the full model). Second, and more importantly, we use a parametric bootstrap of the full model to generate a confidence interval for the coefficient. This package is supplied in the R system for statistical computing (The R Development Core Team,). For a comparison with more traditional methods, we also include the results for repeated-measures multiple regression analysis (rmMRA). Performing an rmMRA is simple: Multiple linear regressions are performed separately for each subject, then a *t* test can be performed to determine if the mean of a coefficient value across subjects, is significantly different from zero.

2.5.5 | Mean P1 latencies and the correlations between P1 latency and RT

We examined if P1 latency decayed with ISI and whether this could be described by the decay function described in Section 2.5.3. P1 latencies were the timing of the maximum positive peak extracted from 50 to 170 ms time window at the O1 electrode. We chose O1 because most of the maximum P1s occurred at O1 and O2, and O1 is on the left hemisphere, the same hemisphere as P7. Next, we

performed the same correlation analysis on P1 latency and median RT using the methods in Section 2.5.4 for N1 latency and RT. Finally, we analysed whether N1 latency could account for the RT more than P1 latency by comparing LMMs correlating P1 latency and RT with or without taking N1 latency as a fixed effect.

3 | RESULTS

3.1 | Gap-metric functions

Our main data are mean ERP of electrode P7 for each condition and each subject. A visual summary for each subject can be constructed by what we call a "firecracker plot": ERP stacked vertically across conditions (in order of gap), and colour-coded for amplitude. The firecracker plot for subject 1 is shown in Figure 3 (code for producing this firecracker plot is available on Github: https://github.com/SourCherries/firecracker). Firecracker plots for the remainder of subjects can be found in Supplementary Figure 1). A large time course, from −800 to 600 ms is shown, so that one can see responses to both masking and target stimuli. The main observation is a systematic change in shape and overall timing from the N170 condition to the widest gap, and then to smaller and smaller gaps: as a mask is introduced and its temporal proximity to the target increases, the neural response to the target appears to delay and widen proportionally. We can quantify these relations more precisely by examining the relation between gap (ms) and N1 peak latency (ms), N1 single-trial jitter (SD ms), and RT (ms).

Each gap function (N1 latency, jitter, and RT), measured separately for each subject, is normalised by its respective value for the N170 condition. We do this because the N170 does not have a "gap," since there is no mask in that condition (arguably, "gap" is effectively infinity). Normalisation is also a way to easily check if values are different from their natural baseline (N170): latencies should be mostly

above 0, as with jitter values and RT. For RT, RT is the medians. And for jitter, which are in units of median absolute deviation (ms), we take the log of jitter divided by N170-jitter.

Gap-metric functions for N1 latency, jitter, and RT, are shown in Figure 4. For each subject, N1 latencies and jitters are a clear exponential function of gap. There are also clear individual differences in decay rate, so we order gap functions for latency and jitter from subjects with the smallest to the highest decay rates (from high k to small k), which are related by a power function between latency and jitter (Figure 5). Therefore, N1 jitter and latency seem to decay "together," but interpretation for this result should be cautious due to the small sample size. Gap-metric functions for jitter of SD and mean RT are shown in Supplementary Figure 2.

Figure 4 also shows a clear trend for an inverse relation between RT and gap (lines are fit here instead of exponential functions, and subjects are ordered by the decay rate [k] of the target N1 latency). RT is more closely examined in the next section.

The width of a deflection in trial-averaged ERP may reflect variability in the exact latency of the corresponding single-trial peaks (jitter). That is the assumption about N1 deflections that we make in this study, which has been supported by previous research (Navajas et al., 2013). However, the width of the N1 in our trial-averaged ERP may instead reflect single-trial peaks with the same width but very little variance in latency. To further confirm that the jitters are the main factor that widen the target N1s, we removed the variance of the single trial latencies by aligning the single-trial peaks then averaged the trials that belong to each condition (Figure 6 shows average N1 after aligning single-trial peaks for subject 1). All the average N1s appeared to have similar width after removing the single trial jitters (Supplement Figure 3).

In agreement with the studies in our survey (Figure 1), our results (Figures 3, 4, and 6) show that the forward-mask changes the timing of the N1 waveform, depending on how close it is to the target image: the smaller the gap, the greater the change in N1 (both delay and
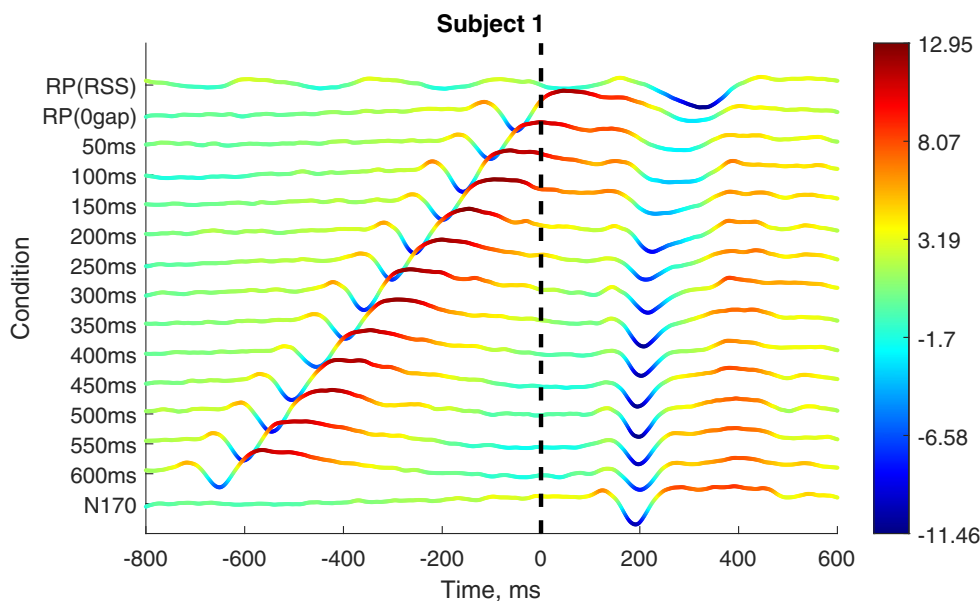

FIGURE 3 Event-related potential (ERP) firecracker plot for subject 1. Mean ERPs measured from P7 are stacked vertically across conditions and voltage is colour-coded, with a corresponding colour bar to the right
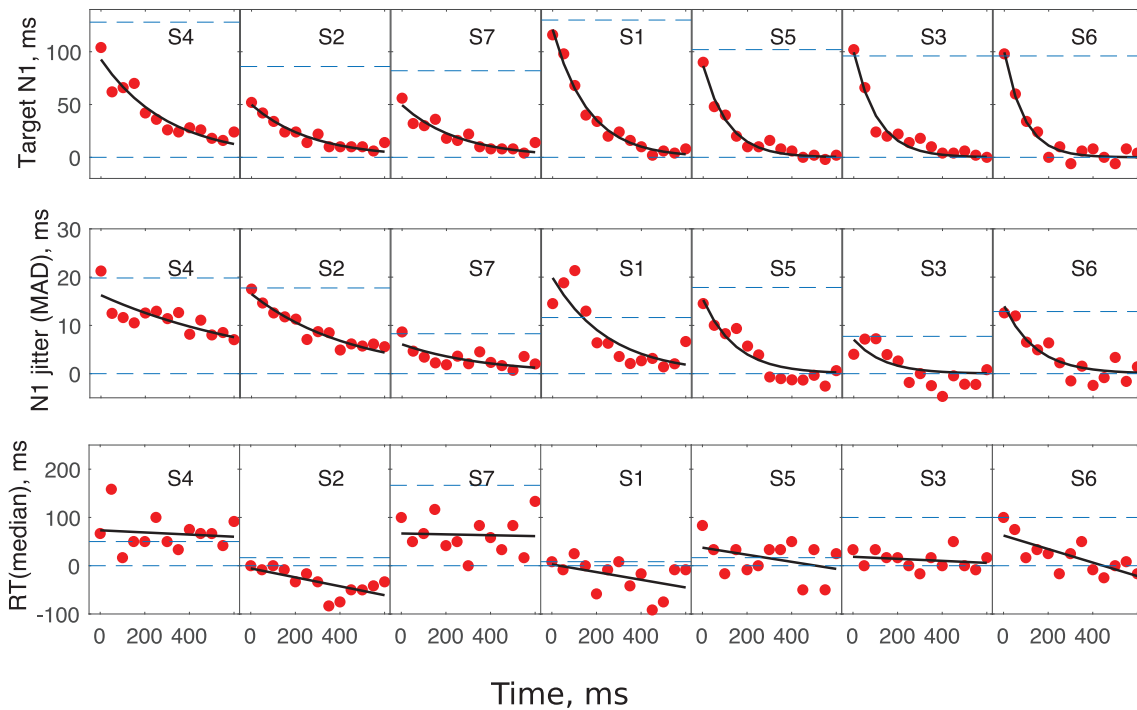
FIGURE 4 Gap functions for N1 latency, N1 jitter (median absolute deviation [MAD]) and median reaction time (RT), from top to bottom. The upper dash lines represent recognition potential (RP) (rapid stream stimulation [RSS] condition), and the bottom dash lines represent N170 (no forward mask condition). The results are ordered by the decay rate (k) of the target N1 latency of the subjects, from big k to small k
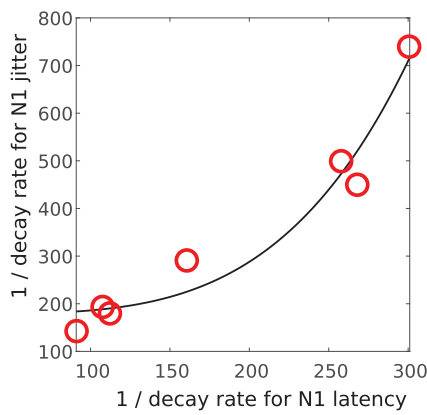

FIGURE 5 Scatter plot of decay rates of N1 latency and jitter (median absolute deviation [MAD]). The latency and jitter were measured from P7

FIGURE 6 Average N1 after aligning single-trial peaks for subject 1. The top panel is the original event-related potentials (ERPs) (15 conditions are plotted on the same y-axis) at P7, the bottom panel is the corresponding ERPs that the single-trial peaks for each condition were aligned to a same time point (the N1 latency in rapid stream stimulation [RSS] condition) before averaging

widening). If that is true, then one would also expect that the speed of a subject's own neural response to the mask—as an intermediate event between mask and target—would have a similar effect: if their mask-N1 is very slow (long latency) then their "effective gap" is much smaller than the "nominal gap" value; but if their mask-N1 is very rapid (short latency) then their "effective gap" is closer to the "nominal gap" between mask- and target-image onsets. Therefore, individual differences in mask-N1 latency should predict individual differences in target-N1 decay rates. The scatterplots in Figure 7 are a first attempt at exploring this relationship. Consistent with our line of

thinking, there appears to be a negative correlation between the individual differences in decay rate, for both N1 latency and jitter, and the latency of a subject's N1 response to the masking stimuli. However, we cannot draw a firm conclusion considering that the small sample size is small.

3.2 | N1 latency and RT

We employ both a LMM and rmMRA. For LMM, we perform two model comparisons. First, we compare subject-intercept only, versus subject-intercept plus N1-latency, with RT as the dependent variable. These models are not nested; they have different fixed-effect structures. Therefore, we estimate these models using maximum likelihood estimation rather than restricted maximum likelihood (Knoblauch & Maloney, 2012). An LMM without N1-latency fits significantly worse than the complete model, with a delta-Chi-square (1 df) = 19.18, p < .001, for the decrease in log likelihood. Similarly, rmMRA results (summarised in Table 2, along with result for the full LMM model), demonstrate a significant N1-latency and RT correlation. An additional nested, model comparison, that examined the effect of including random slopes was inconclusive, with a delta-Chi-square (1 df) = 0, p = 1. Evaluation of the N1-latency and RT correlation can be made on the significance of the LMM model comparison, and the rmMRA. However, p-values obtained from model comparisons of LMM (Knoblauch & Maloney, 2012), and from rmMRA (Baayen, Davidson, & Bates, 2008), tend to be liberal, so we focus mainly on the confidence intervals of effects, which are based on a parametric bootstrap of 1,000 samples from our model based on N1-latency and random subject intercepts (using restricted maximum likelihood). The 95% confidence interval for the coefficient for N1-latency is [0.309, 0.796]. The point estimate (shown in Table 2) is 0.56, so for every 10 ms delay in N1, we expect a delay in RT of about 5 and 6 ms. Note that we used median as the central tendency of RT in the main text because if the goal is to accurately estimate the central tendency of a RT distribution, while protecting against the influence of skewness and outliers, the median is far more efficient than the mean (Wilcox & Rousselet, 2018). Result using mean RT can be found in the Supplementary Table 2.

3.3 | N1 and VPP latencies

In the N170 literature, the VPP component is sometimes measured alongside the N170 component. Joyce and Rossion (2005) find that the amplitudes of the N170 and VPP components vary in a precisely inverse manner and the peaks of the N170 and VPP are temporally coincident. If the N170 latencies were delayed by the forward mask, VPP latencies should also be delayed along with the N170 latencies; as with the timing of every pair of N1 and VPP in each gap condition. In other words, the N170 latencies should correlate with the VPP latencies, as shown by the LMM below.

For LMM, first, we compare subject-intercept only, versus subject-intercept plus VPP-latency. We estimate these models using maximum likelihood estimation. An LMM without VPP-latency fits significantly worse than the complete model, with a delta-Chi-square (1 df) = 173.7, p < .001, for the decrease in log likelihood. Similarly, rmMRA results (summarised in Table 3, along with result for the full LMM model), demonstrate a significant VPP-latency and N1-latency correlation. An additional nested, model comparison, that examined the effect of including random slopes was inconclusive, with a delta-Chi-square (1 df) = 2.06, p = .15. Evaluation of the VPP- and N1-latency correlation can be made on the significance of the LMM model comparison, and the rmMRA. Focussing on our LMM of N1-latency, based on VPP latency and random subject intercepts, we perform a parametric bootstrap of 1,000 samples (using restricted maximum likelihood). The 95% confidence interval for N1-latency is [0.79, 0.94].

3.4 | Topographies

Analysis described here measures matches in topographical distributions between time frames, and between conditions. Inner products were used instead of (normalised) correlations because measuring correlation would require centring and normalising each topography on a frame-by-frame basis. However, such normalisation, we argue, would throw away information about changes in polarity across time, as well as overall voltage energy.

Assuming the N1 topography from the N170 condition is a unique marker associated with processing at N1 (Maurer et al., 2005), the strength of its inner product with topographies from other gap
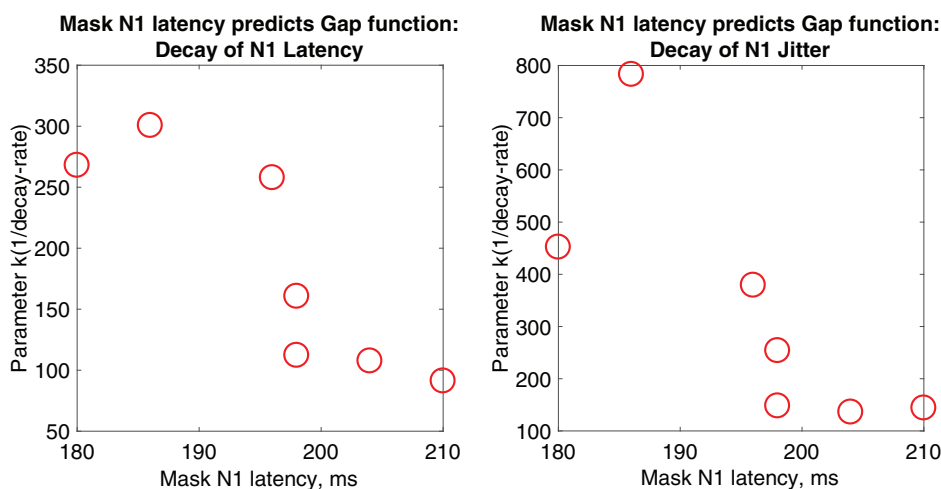

FIGURE 7 Latency of N1 response to masking stimulus predicts k-parameter (1/decay-rate) of target-N1, for both N1 latency and N1 jitter (median absolute deviation [MAD]). The latencies and jitter were measured from P7

TABLE 2 Summary of fixed effects for both LMM (using restricted maximum likelihood) and rmMRA models of RT, predicted by N1-latency. *t* > 2.45 is significant at 5% level (two-tailed)

	LMM			rmMRA		
	Coefficient	SE	t	Coefficient	SE	t
Median RT (ms)	514.75	34.48	14.93	488.38	43.33	11.27
N1 latency (ms)	0.56	0.12	4.64	0.68	0.14	4.74

Abbreviations: LMM, linear mixed model; rmMRA, repeated-measures multiple regression analysis; RT, reaction time.

TABLE 3 Summary of fixed effects for both LMM (using restricted maximum likelihood) and rmMRA models of N1-latency, predicted by VPP-latency. *t* > 2.45 is significant at 5% level (two-tailed)

	LMM			rmMRA		
	Coefficient	SE	t	Coefficient	SE	t
Mean N1 latency (ms)	31.521	8.944	3.524	34.78	17.081	2.04
VPP latency (ms)	0.862	0.038	22.458	0.84	0.082	10.32

Abbreviations: LMM, linear mixed model; rmMRA, repeated-measures multiple regression analysis; VPP, vertex positive potential.

conditions should roughly predict the timing of the N1 in those conditions. How well are N1 latencies in each gap condition predicted by their topographical match with the N170 condition at N1?

In each gap condition, we measured the time course of inner products between the N1 topography from the N170 condition to all other topographies in that condition. If the N1 peak is similar across gap conditions, in the sense that it reflects the same process that underlies the N1 in the N170 condition, then latency of the maximum inner product (MIP) along the time course for a given gap condition should roughly match the timing of the N1 in that condition. In addition, this logic also applies to the RSS condition. To be clear about this analysis, we include markers in Figure 8a that depicts both the timing of N1 latency (red triangles), and the timing of the MIP with N170 topography (black, upside down triangles) for one subject (Subject 1). One can clearly see that maximum latencies follow N1 latencies across gap condition, and that the topographies at N1 latency and MIP latency (Figure 8b) are visually similar across conditions. Time course of inner products for the remainder of subjects can be found in Supplementary Figure 4. To visualise this correlation for every subject, we include a scatter plot between MIP and N1 latencies in Figure 9, using different coloured markers for each of the seven subjects. This plot is convincing: across gap and subject, topographical distributions across time are most similar to the N170 topography at the latency of the N1. To precisely quantify the correlation between N1 latency and the latency of MIP, we performed an LMM, and compared subject-intercept only, versus subject-intercept plus the latency of MIP. An LMM without MIP fits significantly worse than the complete model, with a delta-Chi-square (1 *df*) = 243.56, *p* < .001, for the decrease in log likelihood. Likewise, rmMRA results (summarised in Table 4, along with result for the full LMM model), demonstrate a significant MIP-latency and N1-latency correlation. The 95% confidence interval for the coefficient for MIP-latency is [0.90, 1.02]. The point estimate (shown in Table 4) is 0.96, so for every 10 ms delay in MIP, we expect a delay in N1 around 9.6 ms.

The same analysis was done to match the RP (RSS condition) topography at RP latency with every frame of every condition. The question is similar: are topographies in each gap condition most similar to the RP topography at their respective N1 latencies? The answer to the question is yes. The results using RP topography are basically identical with the results using N170 topography; the RP version of Figures 7 and 8 can be found in the supplementary material (Supplementary Figure 5 and 6).

3.5 | P1 latency and RT

Thierry et al. (2007a, 2007b) and Dering et al. (2011) have found a dissociation between P1 and N170 in category-selectivity. If forward masks lead to delays of N1 latency, does the delay happen as early as P1? Answering this question could provide substantial interpretative implications for visual perception. By visually inspecting Figure 3 and Supplementary Figure 1, it appears that the P1 in the small-gap conditions 50 ms, 0 ms and RSS cannot be reliably isolated from brain response to the forward mask. Therefore, these conditions were excluded from all the analyses on P1. We plotted P1 latency in the same range of y-axis (Figure 10a) as N1 latency in Figure 4 for comparison with N1 latency decay, and the increase of P1 latency from large to small gap is not as drastic as the increase of N1 latency. The decay function (Section 2.5.3) fits the decay of P1 latency poorly for some subjects such as S1, S3, and S6 (Figure 10a, top), due to the noisiness of latencies. Considering that the P1 latency, we extracted could be more or less influenced by forward masks, for comparison, we utilised the topography of P1 in the N170 condition (thus unaffected by the masks) to find the MIP in all the conditions (Figure 10a, bottom; Figure 10b and Supplementary Figure 7). The estimated P1 latency (i.e., MIP latency) exhibits a similar pattern with P1 latency extracted using the maximum peak (Figure 10a).
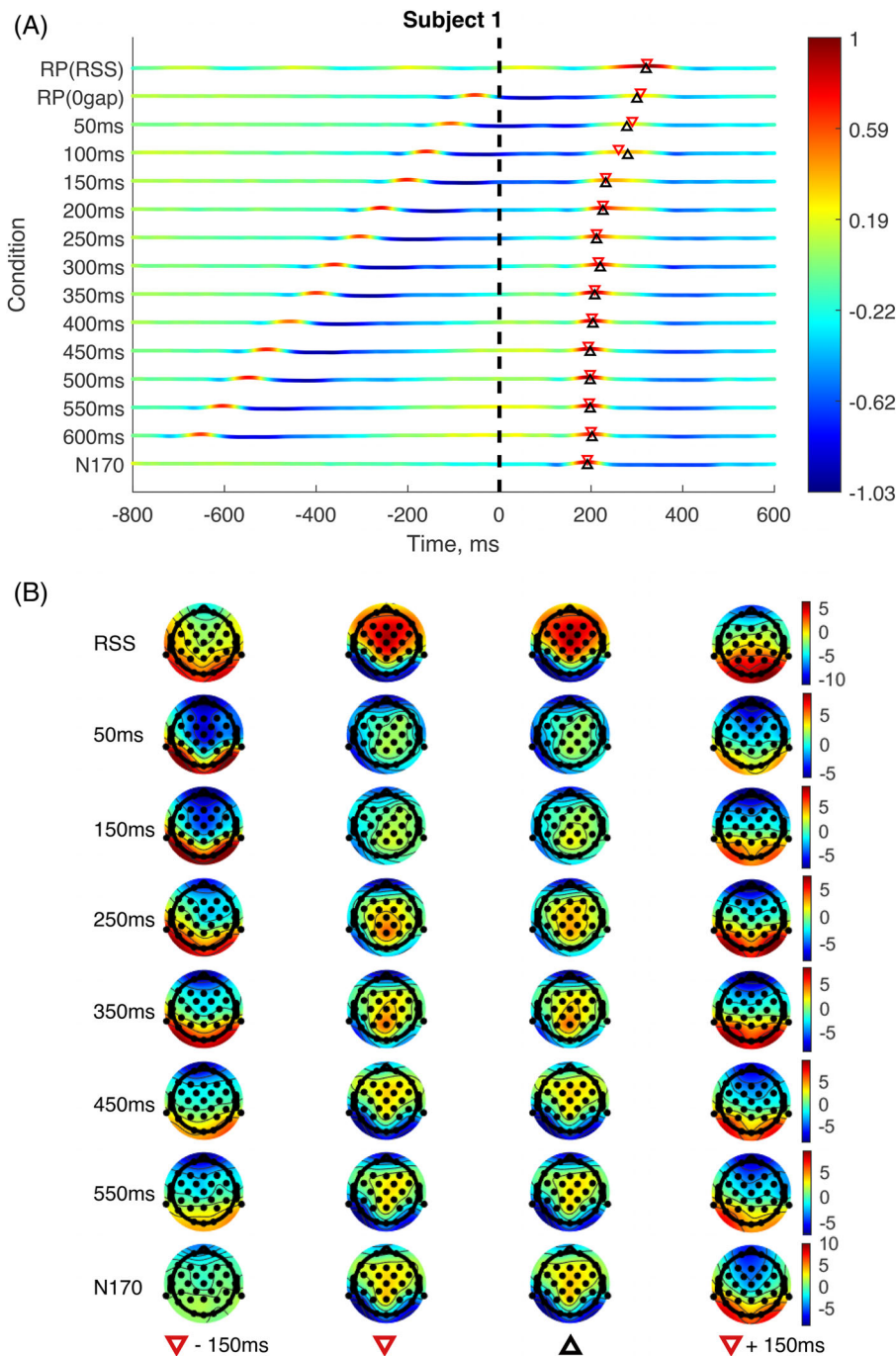
FIGURE 8 (a) Time course of inner product between N170 topographical distribution (at N1 latency, measured from P7), and topographies at every other time frame, and condition. To improve visualisation, each inner-product time course is normalised by its maximum inner product (MIP). In each condition, a red triangle (pointing down) shows the latency of the N1 for the mean event-related potential (ERP) in that condition; and a black triangle (pointing up) shows the latency of the topography in that condition which has the highest inner product with the N170 topography (at N1), within 0–400 ms. According to our hypothesis, black and red triangles should roughly match up. (b) Topographies of N1 latencies and the MIP latencies. The topographies were extracted from the time pointed by the red (the second column) and black (the third column) triangles in Figure 8a. The topographies 150 ms before and after the N1 latency serve as a comparison. To avoid cluttering and oversize the figure, we draw one line of topographies for every other condition

Can P1 predict RT as well? To answer this question, we performed an LMM and a rmMRA model. An LMM without P1-latency fits significantly worse than the complete model, with a delta-Chi-square $(1\ df) = 5.23$, $p = .022$, for the decrease in log likelihood. An additional nested, model comparison, that examined the effect of including random slopes was inconclusive, with a delta-Chi-square $(1\ df) = 0$, $p = 1$. The 95% confidence interval for the coefficient for P1-latency is [0.038, 1.117]. The point estimate (shown in Table 5) is 0.58, so for every 10 ms delay in P1, we expect a delay in RT around 6 ms. Result using mean RT can be found in the Supplementary Table 3.

3.6 | Can N1 predict RT above and beyond what is predicted by P1?

As mentioned above, our results show that both N1 and P1 latency can predict RT. And N1 latency might account for more RT delay than P1 latency. To test this, we applied an LMM. An LMM without N1-latency fits significantly worse than the complete model, with a delta-Chi-square $(1\ df) = 4.1947$, $p = .04055$, for the decrease in log likelihood. The 95% confidence interval for the coefficient for P1-latency is [0.14, 1.08], and for N1-latency is [0.34, 1.63] (Table 6). Result using mean RT can be found in the Supplementary Table 4.

4 | DISCUSSION

The current study tested the hypothesis that the N170 can be nudged forward by forward masking into a component that is morphologically equivalent to an RP. All aspects of waveform morphology revealed a full picture of how ISIs and forward masks influence the target N1 and therefore provided compelling evidence that: (a) the delayed N1 can be recognised as N170; and (b) RP is a delayed version of N170. For each subject, N1 latency fell from its highest level in the zero-gap (quasi-RP) condition, towards the asymptotic level given by the latency in the no-mask (N170) condition. Individual differences in the decay parameter were well predicted by how quickly their mask-evoked N1 occurred: Faster N1 responses to the mask resulted in slower decay rates. Single-trial N1 jitter, our approximation of N1 width, behaved in the same manner as N1 latency: for each subject, an exponential decay with gap increases; and decay parameters well predicted by latency of mask-evoked N1. Target N1 of all the conditions had similar width after removing single-trial N1 jitter. Importantly, RTs were also delayed by gap reductions, and were significantly correlated with N1 latency, consistent with the idea that a delayed N1 signals a delay in information processing. Finally, we
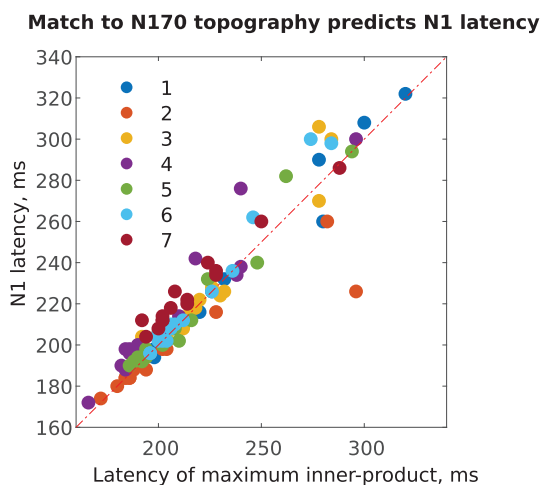
demonstrate that the specific topographical distribution of voltage at N1, measured in the N170 condition, is both unique to the N1 time point in that condition, and best matched to a small temporal window around the N1 time point, for every gap condition and RSS condition (typical RP): (a) topographical similarity to the N170 (at N1) follows the delay in N1 latency as the gap between mask and target narrows and (b) topographical similarity to the N170 in the RSS condition appears at same time as the latency of the typical RP.

4.1 | The delayed N170 should be categorised as N170

The finely spaced gap conditions spanning 0–600 ms allowed us to uncover a continuum of changes in N1 latency and peak width. In agreement with the results of the studies using the short ISIs summarised in our introduction, our results showed that target N1 was delayed when a short ISI was used. Moreover, the width of target N1 was widest and noisiest for the smallest gap, in line with Su et al. (2012). Both latency delay and the wider width can be explained by short ISIs and forward masks using an exponential decay function. When we removed the jitter and aligned the single-trial peak, the N1 widths of different conditions were actually similar (Figure 6), indicating that the single-trial jitter was the main cause of the widened width of N1.

In addition to the studies summarised in Figure 1, of which four studies utilised adaptation (Cao et al., 2014; Fu et al., 2012; Kuehl et al., 2013; Shen et al., 2017), many other N170 studies have adopted short ISI, such as studies using priming (Campanella et al., 2000; Jemel, Pisani, Calabria, Crommelinck, & Bruyer, 2003) and rapid serial visual presentation (RSVP) (Gao et al., 2011; Luo, Feng, He, Wang, & Luo, 2010; Luo et al., 2013; Robinson, Plaut, & Behrmann, 2017). If the N1 latency was out of the typical N170 time window (as almost all these RSVP studies have shown), these studies would have faced one problem, that is: when did the measured effect actually happen? At ~170 ms where the typical N170 occurs? Or at the actual latency the effect was measured? This question is difficult to answer based only on the results of these prior studies. Even if the topography of the N1 seemed similar with the topography of a typical N170 (Gao et al., 2011; Luo et al., 2010, 2013), there was no evidence supporting the idea that the N1 was merely pushed forward by the previous stimulus, and that the topography was not by chance akin to N170. Now our current study has provided this missing evidence.

Match to N170 topography predicts N1 latency

FIGURE 9 The latency of maximum inner product (MIP) with N170 topography for each gap condition, predicts the N1 latency at P7 for that condition, for each subject. For clarity, note that, the x-axis here corresponds to the black triangles depicted in Figure 7 (for subjects S1), while the y-axis corresponds to the red triangles in that figure

TABLE 4 Summary of fixed effects for both LMM (using restricted maximum likelihood) and rmRMA models of N1 latency, predicted by the latency of MIP. t > 2.45 is significant at 5% level (two-tailed)

	LMM			rmMRA		
	Coefficient	SE	t	Coefficient	SE	t
Intercept	11.81	6.96	1.698	7.67	15.79	0.49
MIP latency (ms)	0.96	0.03	31.59	0.97	0.08	12.18

Abbreviations: LMM, linear mixed model; MIP, maximum inner product; rmMRA, repeated-measures multiple regression analysis.
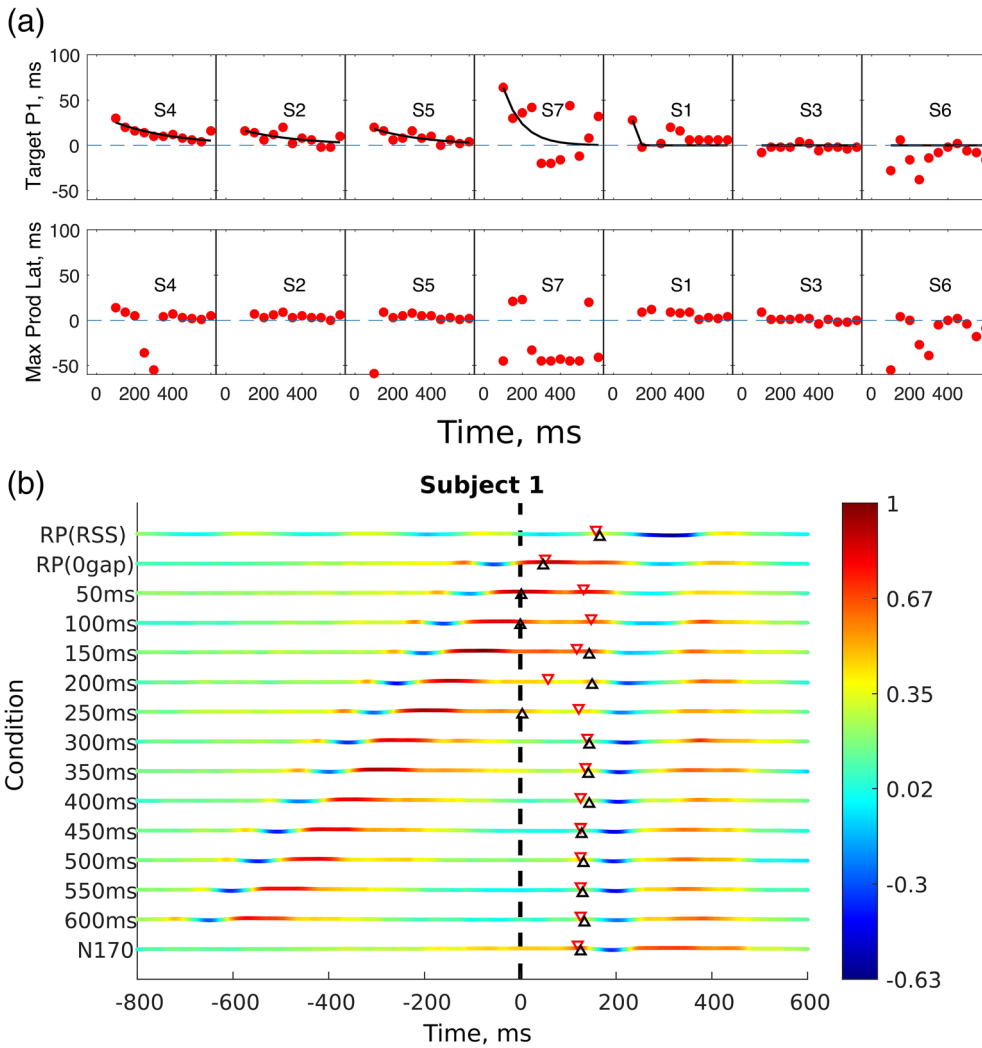
(a)

(b)

FIGURE 10 (a) P1 latency. Top panel is gap functions for P1 latency at O1. The dash lines represent P1 latency of N170 condition (no forward mask condition). The results are ordered by the decay rate (*k*) of the target N1 latency of the subjects, from big *k* to small *k*. Bottom panel, the maximum inner-product (MIP) latency measured by applying dot product between P1 of N170 condition with all the conditions. (b) Time course of inner product between P1 topographical distribution (at P1 latency in N170 condition, measured from O1), and topographies at every other time frame, and condition. Each inner-product time course is normalised by its MIP. In each condition, a red triangle (pointing down) shows the latency of the P1 for the mean event-related potential (ERP) in that condition; and a black triangle (pointing up) shows the latency of the topography in that condition which has the highest inner-product with the P1 topography (at P1), within 0–200 ms

TABLE 5 Summary of fixed effects for both LMM (using restricted maximum likelihood) and rmRMA models of median RT, predicted by the latency of P1 latency. *t* > 2.45 is significant at 5% level (two-tailed)

	LMM			rmMRA		
	Coefficient	**SE**	**t**	**Coefficient**	**SE**	**t**
Intercept	557.45	36.74	15.17	483.9	77.84	6.22
MIP latency (ms)	0.58	0.25	2.33	1.10	0.65	1.77

Abbreviations: LMM, linear mixed model; MIP, maximum inner product; rmMRA, repeated-measures multiple regression analysis; RT, reaction time.

TABLE 6 Summary of fixed effects for both LMM (using restricted maximum likelihood) of median RT, predicted by the latency of P1, and latency of both P1 and N1. *t* > 2.45 is significant at 5% level (two-tailed)

	LMM		
	Coefficient	**SE**	**t**
Intercept	429.4	70.44	6.1
P1 latency (ms)	0.51	0.25	2.1
N1 latency (ms)	0.67	0.32	2.09

Abbreviations: LMM, linear mixed model; RT, reaction time.

4.2 | RP is a delayed version of N170

In order to determine if RP is a delayed version of the N170, we measured RP in both the zero-gap condition (with one forward mask, analogous to Dien et al., 2013) and the RSS condition. The former allowed us to determine if RP was really a delayed response, for the zero-gap condition was the end of the continuum of the gap conditions. The latter condition, employing RSS, confirmed that the delayed N1 was same as the typical RP, as the topographical similarity result showed (Figures 8 and 9 and Supplementary Figures 3–6). Therefore, the results from both conditions have provided the

proper evidence for determining whether RP is a delayed version of the N170.

There are a number of implications for an ambiguity between N170 and RP components. Differently labelled components with different latencies are often assumed to reflect different levels of processing. This can be seen in one review that has included RP and N170: Due to latency differences, Dien (2009) relates RP and N170 to different stages in word processing. However, our results now provide us with greater reason to question interpretations like this: Perhaps the same stage of processing was reflected by both components, only with a change in latency. Another implication of RP-N170 ambiguity is that the semantic processing often associated with RP may prove to be more important to the N170 than is realised in that literature. Most N170 studies focus on the unique visual attributes of a stimulus-category that are often associated with experts. Nonetheless, name-object associations have been found to significantly modulate N170 amplitudes (Heisz & Shedden, 2009); consistent with the idea that the boundary between RP and N170 processing is quite vague. Nonetheless, none of this would be surprising on a physiological level, since we already know that single-cell responses in human IT, believed to underlie much of N170, are sensitive to both visual and semantic attributes (Quiroga, Reddy, Kreiman, Koch, & Fried, 2005). Finally, RP is often described as being more selective for differences in object category, especially familiarity (Martín-Loeches, 2007). While this was mostly conjecture in the past, we have recently shown that, in some conditions, the use of a forward mask can amplify N1-amplitude differences between stimulus categories (Luo et al., 2019). If N170 and RP are not as different as previously thought, then the advantage of using forward masking as a tool to enhance differential responses should be explored in a wider range studies, especially those in the area of expert object recognition.

This ERP/N170 paper is unusual in that, instead of focusing on stimulus selectivity, we focus on waveform morphology: component latency, width, and topographical distribution. Our parametric manipulation of mask-to-target SOA (gap) allowed us to precisely measure a gradual, continuous change in these morphological features between the opposite ends of what are considered to be "N170" and "RP" conditions. And while the systematic transition between "N170" and "RP" is consistent with the idea that the RP is a delayed version of the N170, form does not necessarily follow from function—the underlying processing reflected by N170 and RP. Nonetheless, we remain optimistic, based on two results. First, our correlation between N1 latency and RT suggests that delays in N1 are delays in information processing. Second, we show in another study that the RP and N170 share the same stimulus selectivity in three different types of stimulus-category contrasts (Luo et al., 2019). This is an important first step. Ideally, the time course (and channel distribution) of information processing should be inferred from the data rather than simply assumed to occur at the latencies of pre-defined components (Rousselet et al., 2010; Rousselet & Pernet, 2011);. By taking such an approach, one can determine if ERP sensitivity to stimulus information truly occurs where we expect it to: near the N1 or RP component, depending on the presence of a forward mask and its temporal proximity to the target stimulus. However, that would require a different, more ambitious experimental design, requiring many more trials, and using meaningful stimulus variations that we expect the visual brain to be sensitive to.

One can argue that neither the RSS paradigm nor forward masking are essential for obtaining RP, they are just tools to amplify RP more effectively (Martín-Loeches, 2007). Let us take a closer look into the RP studies that did not use forward masks. First, in the first RP study by Rudell (1991), the RP with 250 ms latency was a difference wave derived from the subtraction between the target condition presenting one target image on each trial and the control condition displaying only a meaningless image on each trial. This genuine 250 ms RP was, obviously, different from the RP delayed by the forward mask(s). Second, Marí-Beffa, Valdés, Cullen, Catena, and Houghton (2005) did not use forward masks and yet claimed they were measuring RP. However, the latency of their RP, at about 200 ms, was in the range of N170 latency. Last but not least, the RP observed by Proverbio and Riva (2009), who did not use forward masks as well, was in fact the second negative defection, unlike the other RP that was the first. In short, the RPs that were measured without forward masks were either indistinguishable from N170 or distinguishable from the RP measured with forward masks. Since the RP reported by Rudell (see Peter Rudell, 1992; Rudell, 1991; Rudell, 1999; Rudell & Hu, 2010; Rudell & Hua, 1996) was actually a positive wave instead of N1, was that RP also a delayed brain signal? The answer is yes, as long as forward masks were used. Besides, the reason why that RP was a positive wave might be due to the bipolar recording Rudell used.

4.3 | Implications for visual processing

4.3.1 | Error-signal hypothesis

Forward masks can evoke recurrent processing that may continue to exert influence on N1-related processes as the target image is presented (Mohsenzadeh, Qin, Cichy, & Pantazis, 2018). That recurrent activity may represent an expectation of scrambled characters that fails to match the real Chinese characters we display as targets (Dux, Visser, Goodhew, & Lipp, 2010; Enns & Di Lollo, 2000). That error may take time for the brain to resolve, leading to a delay in overall processing. This provides one explanation for the relation between ISI and N1 latency that we present in this study, as shorter ISI provide greater opportunity for recurrent processing to exert its effects on downstream, N1-related processes.

4.3.2 | Attentional-capture hypothesis

Stimulus presentations in our study, like in most ERP studies, have rapid onsets and offsets. Our forward masks may strongly capture attention and make it more difficult to release attention for processing of the subsequent target stimulus.

Therefore, it is possible that the delays in visual processing we observe in our study are the result of an attentional mechanism that takes time to release from the lower-level representation of the masking stimulus (Shapiro et al., 1997; Grandison et al., 1997; Mohsenzadeh et al., 2018; Robinson et al., 2019). In support of this explanation, attention can be exogenously redirected to various image properties outside of spatial location, like task-irrelevant visual motion, for example (Arend, Johnston, & Shapiro, 2006; Olivers, 2004).

4.3.3 | Spatial frequency hypothesis

We propose one additional mechanism for mask-induced delay, which focusses solely on the possible effect of masking on the low-level information available to early spatial vision. Hansen, Johnson and Ellemberg (2012) measured the effect of spatial-frequency content on P1 and N1 responses to images of natural scenes. Most relevant to our study is their focus on images with high structural complexity, a subset of natural scenes selected because they have a high concentration of lines and edges. While the natural scenes they use are different from our Chinese characters in many respects, scenes with high structural complexity share with characters a preponderance of edges. In their Experiment 3, Hansen, Johnson and Ellemberg (2012) manipulate the cutoff of a low-pass filter applied to these images, and clearly show a gradual delay in N1 latency as the cutoff lowers (i.e., more N1 delay as frequency components are removed from the highest available); see Figure 6b in their paper. Interestingly, there is no clear change in P1 latency across these frequency conditions, which mirrors the less reliable modulation of P1 latency with ISI in our study. How might frequency content in their study and mask ISI in our study be related? It is possible that mask and target images are perceptually integrated, and that this integration is more likely to happen at shorter ISI. The combined mask-plus-target image may blur out the edges that define a Chinese character just as low-pass filtering would do.

4.3.4 | Deciding between hypotheses

The error-signal hypothesis has significant weaknesses that the attention hypothesis does not have. First, it seems unlikely that scrambled characters can build a clear enough expectation to generate strong error signals. In contrast, consider an experiment where the mask is the word "eager," followed by a target "oven." That is a highly uncommon sequence in written English, thus likely to generate a large error signal associated with the brain's response to "oven." But in the current study, it is not clear what the brain would expect to see after it perceives scrambled characters. Nonetheless, let us assume that forward masking does delay N1 because of a failed expectation. Under the assumption that preferred stimuli are more unexpected after scrambled characters than non-preferred stimuli, one would expect greater delays for target images that are preferred. Our study only measured N1 responses to

preferred stimuli. In a previous study, however, we found no difference in delay between N1 latency to preferred and non-preferred targets under conditions of masking (Luo et al., 2019). Unfortunately, the attention hypothesis has a major weakness. The attention hypothesis is focused on how masking stimuli might induce N1 delay by forcing us to disengage from an earlier image that strongly engages our attention. However, exogenous attention does not modulate N1 nor P1 latency (Valdes-Sosa et al., 1998). That leaves us with the spatial-frequency hypothesis. This hypothesis is intriguing because it suggests a systematic link between concrete image properties and potential delays in early processing. This is not a notion commonly entertained in the electrophysiological literature on familiar object perception. We propose future study of the N1 and P1 using our gap paradigm together with a parametric manipulation of the frequency content of both mask and target images.

5 | CONCLUSION

In summary, systematic properties of our unique "gap-metric" functions and our time courses of topographical similarity, all suggest that shorter ISI leads to longer N170 latency, in other words, the delayed N1 should still be recognised as N170. The implication of the relationship between ISI and the N170 latency also applies for other visual ERPs, that is if a short ISI is used, the component delay should be taken into account when interpreting the time course of the measured effect. Our study also suggests an effective tool to estimate the N170 latency when the peak is hard to identify (i.e., the topographical similarity measurement with dot product).

Taken together with the results of the gap conditions, the RSS condition further confirmed that the RP waveform is a delayed version of the N170. This implies potential benefits from greater crosstalk between RP and N170 literatures, most especially in how these literatures emphasise different types of information-processing, and in the potential use of forward masks as a tool for enhancing stimulus selectivity of the N170 (Luo et al., 2019). In general, our findings suggest that greater caution should be taken when classifying ERP components based on morphology, and that the effect of specific experimental designs (e.g., ISI, forward masks) on the morphology of these components should be considered when comparing components. But given the flexible nature of component morphology we demonstrate in this study, perhaps morphology-based classification should be replaced or at least validated by data-driven approaches to ERP analysis (e.g., Rousselet et al., 2010; Rousselet & Pernet, 2011).

ORCID

Canhuang Luo https://orcid.org/0000-0002-1426-5232
Wei Chen https://orcid.org/0000-0003-0121-6172
Rufin VanRullen https://orcid.org/0000-0002-3611-7716
Ye Zhang https://orcid.org/0000-0002-8549-8420
Carl Michael Gaspar https://orcid.org/0000-0002-3101-1816

REFERENCES

Arend, I., Johnston, S., & Shapiro, K. (2006). Task-irrelevant visual motion and flicker attenuate the attentional blink. *Psychonomic Bulletin & Review*, *13*(4), 600–607. https://doi.org/10.3758/BF03193969

Baayen, R. H., Davidson, D. J., & Bates, D. M. (2008). Mixed-effects modeling with crossed random effects for subjects and items. *Journal of Memory and Language*, *59*(4), 390–412. https://doi.org/10.1016/j.jml.2007.12.005

Bates, D., Mächler, M., Bolker, B., & Walker, S. (2014). Fitting linear mixed-effects models using lme4. Retrieved from http://arxiv.org/abs/1406.5823

Bentin, S., Mouchetant-Rostaing, Y., Giard, M. H., Echallier, J. F., & Pernier, J. (1999). ERP manifestations of processing printed words at different psycholinguistic levels: Time course and scalp distribution. *Journal of Cognitive Neuroscience*, *11*(3), 235–260. https://doi.org/10.1162/089892999563373

Bentin, S., Allison, T., Puce, A., Perez, E., & McCarthy, G. (1996). Electrophysiological studies of face perception in humans. *Journal of Cognitive Neuroscience*, *8*, 551–565. https://doi.org/10.1162/jocn.1996.8.6.551

Bentin, S., Taylor, M. J., Rousselet, G. A., Itier, R. J., Caldara, R., Schyns, P. G., ... Rossion, B. (2007). Controlling interstimulus perceptual variance does not abolish N170 face sensitivity. *Nature Neuroscience*, *10*(7), 801–802. https://doi.org/10.1038/nn0707-801

Brainard, D. H. (1997). The psychophysics toolbox. *Spatial Vision*, *10*(4), 433–436. https://doi.org/10.1163/156856897X00357

Campanella, S., Hanoteau, C., Depy, D., Rossion, B., Bruyer, R., Crommelinck, M., & Guerit, J. M. (2000). Right N170 modulation in a face discrimination task: An account for categorical perception of familiar faces. *Psychophysiology*, *37*(6), 796–806. https://doi.org/10.1111/1469-8986.3760796

Cao, X. H., Jiang, B., Li, C., & He, Z. Q. (2014). Rapid adaptation effect of N170 for printed words. *Perceptual and Motor Skills*, *119*(1), 191–202. https://doi.org/10.2466/24.22.PMS.119c15z6

Carreiras, M., Armstrong, B. C., Perea, M., & Frost, R. (2014). The what, when, where, and how of visual word recognition. *Trends in Cognitive Sciences*, *18*(2), 90–98. https://doi.org/10.1016/j.tics.2013.11.005

Delorme, A., & Makeig, S. (2004). EEGLAB: An open source toolbox for analysis of single-trial EEG dynamics including independent component analysis. *Journal of Neuroscience Methods*, *134*(1), 9–21. https://doi.org/10.1016/j.jneumeth.2003.10.009

Dering, B., Martin, C. D., Moro, S., Pegna, A. J., & Thierry, G. (2011). Face-sensitive processes one hundred milliseconds after picture onset. *Frontiers in Human Neuroscience*, *5*, 93. https://doi.org/10.3389/fnhum.2011.00093

Dering, B., Martin, C. D., & Thierry, G. (2009). Is the N170 peak of visual event-related brain potentials car-selective? *Neuroreport*, *20*(10), 902–906. https://doi.org/10.1097/WNR.0b013e328327201d

Dien, J., Brian, E. S., Molfese, D. L., & Gold, B. T. (2013). Combined ERP/fMRI evidence for early word recognition effects in the posterior inferior temporal gyrus. *Cortex*, *49*(9), 2307–2321. https://doi.org/10.1016/j.cortex.2013.03.008

Dien, J. (2009). The neurocognitive basis of reading single words as seen through early latency ERPs: A model of converging pathways. *Biological Psychology*, *80*(1), 10–22. https://doi.org/10.1016/j.biopsycho.2008.04.013

Dux, P. E., Visser, T. A. W., Goodhew, S. C., & Lipp, O. V. (2010). Delayed reentrant processing impairs visual awareness: An object-substitution-masking study. *Psychological Science*, *21*(9), 1242–1247. https://doi.org/10.1177/0956797610379866

Eimer, M. (2000). The face-specific N170 component reflects late stages in the structural encoding of faces. *Neuroreport*, *11*(10), 2319–2324. https://doi.org/10.1097/00001756-200007140-00050

Enns, J. T., & Di Lollo, V. (2000). What's new in visual masking? *Trends in Cognitive Sciences*, *4*(9), 345–352. https://doi.org/10.1016/S1364-6613(00)01520-5

Fu, S., Feng, C., Guo, S., Luo, Y., & Parasuraman, R. (2012). Neural adaptation provides evidence for categorical differences in processing of faces and Chinese characters: An ERP study of the N170. *PLoS One*, *7*(7), e41103. https://doi.org/10.1371/journal.pone.0041103

Gao, X., Deng, X., Chen, N., Luo, W., Hu, L., Jackson, T., & Chen, H. (2011). Attentional biases among body-dissatisfied young women: An ERP study with rapid serial visual presentation. *International Journal of Psychophysiology*, *82*(2), 133–142. https://doi.org/10.1016/j.ijpsycho.2011.07.015

Grainger, J., & Holcomb, P. J. (2009). Watching the word go by: On the time-course of component processes in visual word recognition. *Language and Linguistics Compass*, *3*(1), 128–156. https://doi.org/10.1111/j.1749-818X.2008.00121.x

Grandison, T. D., Ghirardelli, T. G., & Egeth, H. E. (1997). Beyond similarity: Masking of the target is sufficient to cause the attentional blink. *Perception and Psychophysics*, *59*(2), 266–274. https://doi.org/10.3758/bf03211894

Hansen, B. C., Johnson, A. P., & Ellemberg, D. (2012). Different spatial frequency bands selectively signal for natural image statistics in the early visual system. *Journal of Neurophysiology*, *108*(8), 2160–2172. https://doi.org/10.1152/jn.00288.2012

Harris, A., & Nakayama, K. (2007). Rapid face-selective adaptation of an early extrastriate component in MEG. *Cerebral Cortex*, *17*(1), 63–70. https://doi.org/10.1093/cercor/bhj124

Harris, J. A., Te Wu, C., & Woldorff, M. G. (2011). Sandwich masking eliminates both visual awareness of faces and face-specific brain activity through a feedforward mechanism. *Journal of Vision*, *11*(7), 1–12. https://doi.org/10.1167/11.7.1

Heisz, J. J., & Shedden, J. M. (2009). Semantic learning modifies perceptual face processing. *Journal of Cognitive Neuroscience*, *21*(6), 1127–1134. https://doi.org/10.1162/jocn.2009.21104

Hinojosa, J. A., Martín-Loeches, M., Gómez-Jarabo, G., & Rubia, F. J. (2000). Common basal extrastriate areas for the semantic processing of words and pictures. *Clinical Neurophysiology*, *111*(3), 552–560. https://doi.org/10.1016/S1388-2457(99)00275-8

Jemel, B., Pisani, M., Calabria, M., Crommelinck, M., & Bruyer, R. (2003). Is the N170 for faces cognitively penetrable? Evidence from repetition priming of Mooney faces of familiar and unfamiliar persons. *Cognitive Brain Research*, *17*(2), 431–446. https://doi.org/10.1016/S0926-6410(03)00145-9

Joyce, C., & Rossion, B. (2005). The face-sensitive N170 and VPP components manifest the same brain processes: The effect of reference electrode site. *Clinical Neurophysiology*, *116*(11), 2613–2631. https://doi.org/10.1016/j.clinph.2005.07.005

Kleiner, M., Brainard, D., Pelli, D., Ingling, A., Murray, R., & Broussard, C. (2007). What's new in psychtoolbox-3. *Perception*, *36*(14), 1–16. https://doi.org/10.1068/v070821

Knoblauch, K., & Maloney, L. T. (2012). *Modeling psychophysical data in R.* New York, NY: Springer. https://doi.org/10.1007/978-1-4614-4475-6

Krafnick, A. J., Tan, L.-H., Flowers, D. L., Luetje, M. M., Napoliello, E. M., Siok, W.-T., ... Eden, G. F. (2016). Chinese character and English word processing in children's ventral occipitotemporal cortex: fMRI evidence for script invariance. *NeuroImage*, 133, 302–312. https://doi.org/10.1016/j.neuroimage.2016.03.021

Kuehl, L. K., Brandt, E. S. L., Hahn, E., Dettling, M., & Neuhaus, A. H. (2013). Exploring the time course of N170 repetition suppression: A preliminary study. *International Journal of Psychophysiology*, 87(2), 183–188. https://doi.org/10.1016/j.ijpsycho.2012.12.007

Libet, B., Gleason, C. A., Wright, E. W., & Pearl, D. K. (1993). Time of conscious intention to act in relation to onset of cerebral activity (readiness-potential). In *Neurophysiology of consciousness*. Contemporary Neuroscientists (Selected Papers of Leaders in Brain Research), Boston, MA: Birkhäuser. https://doi.org/10.1007/978-1-4612-0355-1_15

Lin, S. E., Chen, H. C., Zhao, J., Li, S., He, S., & Weng, X. C. (2011). Left-lateralized N170 response to unpronounceable pseudo but not false Chinese characters-the key role of orthography. *Neuroscience*, 190, 200–206. https://doi.org/10.1016/j.neuroscience.2011.05.071

Lopez-Calderon, J., & Luck, S. J. (2014). ERPLAB: An open-source toolbox for the analysis of event-related potentials. *Frontiers in Human Neuroscience*, 8, 213. https://doi.org/10.3389/fnhum.2014.00213

Luo, C., Chen, W., Zhang, Y., & Gaspar, C. M. (2019). Rapid stream stimulation can enhance the stimulus selectivity of early evoked responses to written characters but not faces. *PLoS One*, 14(3), e0213637. https://doi.org/10.1371/journal.pone.0213637

Luo, W., Feng, W., He, W., Wang, N. Y., & Luo, Y. J. (2010). Three stages of facial expression processing: ERP study with rapid serial visual presentation. *NeuroImage*, 49(2), 1857–1867. https://doi.org/10.1016/j.neuroimage.2009.09.018

Luo, W., He, W., Yang, S., Feng, W., Chen, T., Wang, L., ... Luo, Y. J. (2013). Electrophysiological evidence of facial inversion with rapid serial visual presentation. *Biological Psychology*, 92(2), 395–402. https://doi.org/10.1016/j.biopsycho.2012.11.019

Marí-Beffa, P., Valdés, B., Cullen, D. J. D., Catena, A., & Houghton, G. (2005). ERP analyses of task effects on semantic processing from words. *Cognitive Brain Research*, 23(2–3), 293–305. https://doi.org/10.1016/j.cogbrainres.2004.10.016

Martens, U., Schweinberger, S. R., Kiefer, M., & Burton, A. M. (2006). Masked and unmasked electrophysiological repetition effects of famous faces. *Brain Research*, 1109(1), 146–157. https://doi.org/10.1016/j.brainres.2006.06.066

Martín-Loeches, M. (2007). The gate for reading: Reflections on the recognition potential. *Brain Research Reviews*, 53(1), 89–97. https://doi.org/10.1016/j.brainresrev.2006.07.001

Martín-Loeches, M., Hinojosa, J. A., Fernández-Frías, C., & Rubia, F. J. (2001). Functional differences in the semantic processing of concrete and abstract words. *Neuropsychologia*, 39(10), 1086–1096. https://doi.org/10.1016/S0028-3932(01)00033-1

Martin-Loeches, M., Hinojosa, J. A., Gomez-Jarabo, G., & Rubia, F. J. (2001). An early electrophysiological sign of semantic processing in basal extrastriate areas. *Psychophysiology*, 38(1), 114–124. https://doi.org/10.1111/1469-8986.3810114

Maurer, U. (2008). Category specificity in early perception: Face and word N170 responses differ in both lateralization and habituation properties. *Frontiers in Human Neuroscience*, 2, 18. https://doi.org/10.3389/neuro.09.018.2008

Maurer, U., Brandeis, D., & McCandliss, B. D. (2005). Fast, visual specialization for reading in English revealed by the topography of the N170 ERP response. *Behavioral and Brain Functions*, 1, 13. https://doi.org/10.1186/1744-9081-1-13

Maurer, U., Zevin, J. D., & McCandliss, B. D. (2008). Left-lateralized N170 effects of visual expertise in reading: Evidence from Japanese syllabic and logographic scripts. *Journal of Cognitive Neuroscience*, 20(10), 1878–1891. https://doi.org/10.1162/jocn.2008.20125

Milne, E. (2011). Increased intra-participant variability in children with autistic spectrum disorders: Evidence from single-trial analysis of evoked EEG. *Frontiers in Psychology*, 2, 51. https://doi.org/10.3389/fpsyg.2011.00051

Mohsenzadeh, Y., Qin, S., Cichy, R. M., & Pantazis, D. (2018). Ultra-rapid serial visual presentation reveals dynamics of feedforward and feedback processes in the ventral visual pathway. *eLife*, 7, e36329.

Näätänen, R., Gaillard, A. W. K., & Mäntysalo, S. (1978). Early selective-attention effect on evoked potential reinterpreted. *Acta Psychologica*, 42, 313–329. https://doi.org/10.1016/0001-6918(78)90006-9

Navajas, J., Ahmadi, M., & Quian Quiroga, R. (2013). Uncovering the mechanisms of conscious face perception: A single-trial study of the N170 responses. *Journal of Neuroscience*, 33(4), 1337–1343. https://doi.org/10.1523/JNEUROSCI.1226-12.2013

Olivers, C. N. L. (2004). Blink and shrink: The effect of the attentional blink on spatial processing. *Journal of Experimental Psychology: Human Perception and Performance*, 30(3), 613–631. https://doi.org/10.1037/0096-1523.30.3.613

Peter Rudell, A. (1992). Rapid stream stimulation and the recognition potential. *Electroencephalography and Clinical Neurophysiology*, 83(1), 77–82. https://doi.org/10.1016/0013-4694(92)90135-5

Proverbio, A. M., & Riva, F. (2009). RP and N400 ERP components reflect semantic violations in visual processing of human actions. *Neuroscience Letters*, 459(3), 142–146. https://doi.org/10.1016/j.neulet.2009.05.012

Quiroga, R. Q., Reddy, L., Kreiman, G., Koch, C., & Fried, I. (2005). Invariant visual representation by single neurons in the human brain. *Nature*, 435(7045), 1102–1107. https://doi.org/10.1038/nature03687

R Core Team (2011). *R: A language and environment for statistical computing reference index*. Vienna, Austria. R Foundation for Statistical Computing.

Robinson, A. K., Plaut, D. C., & Behrmann, M. (2017). Word and face processing engage overlapping distributed networks: Evidence from RSVP and EEG investigations. *Journal of Experimental Psychology: General*, 146(7), 943–961. https://doi.org/10.1037/xge0000302

Robinson, A. K., Grootswagers, T., & Carlson, T. A. (2019). The influence of image masking on object representations during rapid serial visual presentation. *NeuroImage*, 197, 224–231. http://dx.doi.org/10.1016/j.neuroimage.2019.04.050

Rousselet, G. A., Gaspar, C. M., Pernet, C. R., Husk, J. S., Bennett, P. J., & Sekuler, A. B. (2010). Healthy aging delays scalp EEG sensitivity to noise in a face discrimination task. *Frontiers in Psychology*, 1, 19. https://doi.org/10.3389/fpsyg.2010.00019

Rousselet, G. A., & Pernet, C. R. (2011). Quantifying the time course of visual object processing using ERPs: It's time to up the game. *Frontiers in Psychology*, 2, 107. https://doi.org/10.3389/fpsyg.2011.00107

Rudell, A. P. (1999). The recognition potential and the word frequency effect at a high rate of word presentation. *Cognitive Brain Research*, 8(2), 173–175. https://doi.org/10.1016/S0926-6410(99)00018-X

Rudell, A. P., & Hu, B. (2010). Effects of long-time reading experience on reaction time and the recognition potential. *International Journal of Psychophysiology*, 76(3), 158–168. https://doi.org/10.1016/j.ijpsycho.2010.03.006

Rudell, A. P., & Hua, J. (1996). The recognition potential and conscious awareness. *Electroencephalography and Clinical Neurophysiology*, 98(4), 309–318. https://doi.org/10.1016/0013-4694(95)00265-0

Rudell, A. P. (1991). The recognition potential contrasted with the P300. *International Journal of Neuroscience*, 60(1), 85–111. https://doi.org/10.3109/00207459109082040

Shapiro K. L., Caldwell J., Sorensen R. E. (1997). Personal names and the attentional blink: A visual "cocktail party" effect. *Journal of*

Experimental Psychology: Human Perception and Performance, *23*(2), 504–514. https://doi.org/10.1037/0096-1523.23.2.504

Shen, C., Stasch, J., Velenosi, L., Madipakkam, A. R., Edemann-Callesen, H., & Neuhaus, A. H. (2017). Face identity is encoded in the duration of N170 adaptation. *Cortex*, *86*, 55–63. https://doi.org/10.1016/j.cortex.2016.10.010

Su, I.-F., Mak, S.-C. C., Cheung, L.-Y. M., & Law, S.-P. (2012). Taking a radical position: Evidence for position-specific radical representations in Chinese character recognition using masked priming ERP. *Frontiers in Psychology*, *3*, 333. https://doi.org/10.3389/fpsyg.2012.00333

Tanaka, J. W., & Curran, T. (2001). A neural basis for expert object recognition. *Psychological Science*, *12*(1), 43–47. https://doi.org/10.1111/1467-9280.00308

Taylor, M. J., Itier, R. J., Allison, T., & Edmonds, G. E. (2001). Direction of gaze effects on early face processing: Eyes-only versus full faces. *Cognitive Brain Research*, *10*(3), 333–340. https://doi.org/10.1016/S0926-6410(00)00051-3

Thierry, G., Martin, C. D., Downing, P. E., & Pegna, A. J. (2007a). Is the N170 sensitive to the human face or to several intertwined perceptual and conceptual factors? *Nature Neuroscience*, *10*(7), 802–803. https://doi.org/10.1038/nn0707-802

Thierry, G., Martin, C. D., Downing, P., & Pegna, A. J. (2007b). Controlling for interstimulus perceptual variance abolishes N170 face selectivity. *Nature Neuroscience*, *10*(4), 505–511. https://doi.org/10.1038/nn1864

Valdes-Sosa, M., Cobo, A., & Pinilla, T. (1998). Transparent motion and object-based attention. *Cognition*, *66*(2), B13–B23. https://doi.org/10.1016/s0010-0277(98)00012-2

Wilcox, R. R., & Rousselet, G. A. (2018). A guide to robust statistical methods in neuroscience. *Current Protocols in Neuroscience*, *82*(1), 8.42.1–8.42.30. http://dx.doi.org/10.1002/cpns.41

Winkler, I., Czigler, I., Sussman, E., Horváth, J., & Balázs, L. (2005). Preattentive binding of auditory and visual stimulus features. *Journal of Cognitive Neuroscience*, *17*, 320–339. https://doi.org/10.1162/0898929053124866

Woodman, G. F. (2010). A brief introduction to the use of event-related potentials in studies of perception and attention. *Attention, Perception, & Psychophysics*, *72*(8), 2031–2046. https://doi.org/10.3758/APP.72.8.2031

Yang, H., Zhao, J., Gaspar, C. M., Chen, W., Tan, Y., & Weng, X. (2017). Selectivity of N170 for visual words in the right hemisphere: Evidence from single-trial analysis. *Psychophysiology*, *54*(8), 1128–1137. http://doi.org/10.1111/psyp.12867

Zhang, D., Luo, W., & Luo, Y. (2013). Single-trial ERP evidence for the three-stage scheme of facial expression processing. *Science China Life Sciences*, *56*(9), 835–847. https://doi.org/10.1007/s11427-013-4527-8

SUPPORTING INFORMATION

Additional supporting information may be found in the online version of the article at the publisher's website.